JAIST Repository
https://dspace.jaist.ac.jp/

Title	A Method to Evaluate Explosive Crystallization Velocity of Amorphous Silicon Films during Flash Lamp Annealing
Author(s)	Ohdaira, Keisuke
Citation	Canadian Journal of Physics, 92(7/8): 718-722
Issue Date	2014-02-25
Type	Journal Article
Text version	author
URL	http://hdl.handle.net/10119/12331
Rights	This is the author's version of a work accepted for publication by NRC Research Press. Keisuke Ohdaira, Canadian Journal of Physics, 92(7/8), 2014, 718-722. http://dx.doi.org/10.1139/cjp-2013-0574
Description	

JAIST
JAPAN ADVANCED INSTITUTE OF SCIENCE AND TECHNOLOGY

Japan Advanced Institute of Science and Technology

A Method to Evaluate Explosive Crystallization Velocity of Amorphous Silicon Films during Flash Lamp Annealing

Keisuke Ohdaira

Japan Advanced Institute of Science and Technology (JAIST)

1-1 Asahidai, Nomi, Ishikawa 923-1292, Japan

e-mail: ohdaira@jaist.ac.jp

Abstract

Flash lamp annealing (FLA) of micrometer-order-thick amorphous silicon (a-Si) films can induce explosive crystallization (EC), high-speed lateral crystallization driven by the release of latent heat. We develop multi-pulse flash lamp annealing (FLA) system, which emits a quasi-millisecond pulse consisting of a number of sub-pulses. The emission frequency of the sub-pulses can be systematically controlled, and the emission of sub-pulses leads to the periodic modulation of the temperature of a Si film and the resulting formation of macroscopic stripe patterns. The relationship between a sub-pulse emission frequency and the width of the macroscopic stripe patterns yields EC velocity. Two kinds of EC modes can be observed, depending on the methods of precursor a-Si deposition and/or a-Si film thickness.

PACS No.: 81.10.Jt, 81.40.Ef, 88.40.jj

1. Introduction

Thin-film crystalline Si (c-Si) is of great interest as a photovoltaic material because of the possibility of high efficiency and efficient material usage. Of a variety of methods to form thin c-Si, the crystallization of precursor amorphous silicon (a-Si) films on low-cost substrates has been expected as a prospective candidate [1-3]. We have investigated the crystallization of a-Si films by flash lamp annealing (FLA), millisecond-order rapid annealing using a pulse light emitted from Xe lamps [4-11]. Due to its proper annealing duration, FLA can realize the sufficient heating of a micrometer-order-thick a-Si film without serious thermal damage onto an entire glass substrate. Another advantage of FLA is large-area, uniform pulse emission without scanning, unlike the cases of laser annealing [12]. FLA can thus be a high-throughput annealing method for the formation of large-area polycrystalline Si (poly-Si) films.

We have so far confirmed that a few μm-thick a-Si films can be crystallized by a single shot of flash pulse [4-6,11]. The mechanism of the flash-lamp-induced crystallization of a-Si films is based on explosive crystallization (EC). EC is an well-known crystallization mode generally seen in amorphous materials with higher enthalpy than crystalline material, showing lateral crystallization driven by the release of latent heat [6,8,9,11,13]. We sometimes observe an EC including solid-phase nucleation (SPN), which leaves behind 1-μm-spacing periodic microstructures [6,8,9], and sometimes see the other type of EC completely governed by liquid-phase epitaxy (LPE), which forms relatively large grains with a length of several tens of μm [9,11]. The evaluation of the velocity of lateral crystallization is thus quite important for the discussion of the fundamental physics of crystallization mechanisms. An *in-situ*

observation system of the EC is, however, generally quite complex and difficult to be equipped in a FLA system.

We have thus established a new method to evaluate EC velocity by using multi-pulse FLA [9]. Multi-pulse FLA can supply a quasi-millisecond pulse consisting of a number of sub-pulses whose emission frequency can be systematically controlled. Si films receive periodic temperature modulation by the sub-pulse emission, and as a result, macroscopic stripe patterns are formed on the surface of poly-Si films. By considering the emission frequency of sub-pulses and the width of the macroscopic stripe patterns, EC velocity is easily estimated, without any complicated *in-situ* observation systems. In this paper, we explain the details of the multi-pulse FLA system, along with thermal simulation to understand how the temperature modulation of Si films is during sub-pulse emission. We also discuss the reason of the emergence of different types of ECs depending on the properties of precursor a-Si films.

2. Simulation and experimental methods

2.1 Thermal simulation

We used a software named "PHOENICS", produced by Concentration Heat and Momentum Limited, for thermal simulation. Figure 1 shows a structure and heating model used for the thermal simulation. As a quasi-5-ms pulse, we assumed a rectangular wave consisting of 20 sub-pulses (emission frequency of 4 kHz) with a duration of 0.2 ms and 0.05 ms intervals between sub-pulses. Fluence of the quasi 5-ms pulse was set to be 6.4 J/cm^2. We used a structure with a 4.5 μm-thick a-Si film on a 500 μm-thick glass substrate for the thermal simulation, which were divided into 20 and 200 meshes, respectively. In the actual FLA, a flash-lamp pulse has a broad

spectrum in a visible range, and not only the surface but the bottom of the a-Si film is heated by absorbing the pulse light. However, since most of light is absorbed in the vicinity of a-Si surface in such a thick film, we approximated the heating of a-Si from a plate put on the surface of the a-Si film. After 5-ms heating, 5-ms cooling time was set in order to know how the temperature of Si decreases rapidly. No phase change (crystallization or melting) is included in the simulation. The initial temperature of the structure was set to be 400 °C.

2.2 Multi-pulse FLA system

Figure 2 shows a FLA equipment used in this study, manufactured by Design System Co., Ltd.. A Xe flash lamp is set at a focal point of an elliptical mirror in a lamp house. The lamp house can be moved between two positions: on a detector and on a process chamber. The irradiance of a flash pulse can be checked by the detector immediately before irradiating the pulse on a sample. The position of the sample is designed to be the other focal point of the elliptical mirror, in order to effectively use the light emitted from the Xe lamp. A sample holder can be heated up to 500 °C by a halogen lamp from the back side of the holder.

Figure 3 shows a photograph of the Xe lamp, produced by ORC Manufacturing Co., Ltd.. The principle of the sub-pulse emission is based on a stroboscopic lamp. A voltage charged in a capacitor up to 1000 V is applied between main electrodes, and a high voltage of 15 kV is applied to a trigger electrode wound around the lamp in order to temporarily reduce an impedance of Xe gas. The emission of discrete sub-pulses can be realized by turning on and off the voltage to the trigger electrode. Figure 4 shows photographs of pulse light seen between the lamp house and the process chamber,

captured using a high-speed camera FASTCAM SA-X2 (Photron), at the moments of turning on and off the trigger voltage. Light intensities in the two cases are obviously different, and the emission of sub-pulses can periodically modulate the temperature of a Si film. It should also be noted that the light emission is not completely vanished at the moment of no voltage application to the trigger electrode.

2.3 Poly-Si formation and characterization

We used 20×20×0.7 mm^3-sized quartz or Eagle XG glass for substrates. We deposited a-Si films by three different methods: sputtering, electron-beam- (EB-) evaporation, and catalytic chemical vapor deposition (Cat-CVD). The thickness of a-Si films was also changed from 2 to 10 μm. Only in the case of Cat-CVD film, sputtered Cr adhesion layers were inserted between a-Si films and glass substrates, in order to suppress Si film peeling during FLA [4]. A substrate temperature during EB-evaporation was set to be 350 °C. The details of other deposition conditions for sputtered, Cat-CVD, and EB-evaporated a-Si films were summarized elsewhere [9]. FLA was performed at a fluence of 10-16 J/cm^2 with a duration of 5-7 ms under Ar flow. A supporting stage preheat temperature was 450-500 °C. The sub-pulse emission frequency was systematically changed from 1 to 10 kHz. Only one shot of FLA was performed for each sample. No dehydrogenation process was performed prior to FLA even for Cat-CVD hydrogenated a-Si films. Lateral EC velocity was estimated by dividing the average width of macroscopic stripe patterns formed by the irradiation of multi-pulse by the inverse of sub-pulse emission frequency. The cross-sectional microstructures of flash-lamp-crystallized (FLC) poly-Si films were observed by transmission electron microscopy (TEM).

3. Results and discussion

3.1 Thermal simulation

Figure 5 shows the result of a thermal simulation for an a-Si/glass structure heated by 4-kHz multi-pulse irradiation. The temperature of an a-Si film increases up to around 1200 °C at 5 ms. On the other hand, only a 50-100 μm-thick region from the surface of a glass substrate is heated by FLA. Due to the selective heating, a glass substrate does not entirely receive a thermal damage. This vertical thermal gradient can also be a cause of cracking in glass substrates, and we need the careful selection of a glass material to suppress glass cracking [10]. It should be emphasized that a fluence of 6.4 J/cm^2 is much smaller than those of actual experimental values of more than 10 J/cm^2. This indicates that considerable amount of pulse light energy is wasted due to reflection and/or transmission. In our previous study, we have shown that a 4.5-μm-thick a-Si film absorbs about only 50% of visible light, and there is no effective absorption of infra-red light [6]. The value of 6.4 J/cm^2 used for the simulation is thus quantitatively reasonable. Time-dependent temperature variations at Si surface, Si bottom (glass surface), and glass bottom are summarized in Fig. 6. The bottom of a glass substrate is not heated at all. The temperature difference between the surface and the bottom of an a-Si film is <60 °C. It should be noted that this temperature difference must be over-estimated, since heating by flash-lamp pulse is now approximated as a heating from a plate on the Si film. Due to the irradiation of discrete sub-pulses, a Si film undergoes a considerable periodic temperature modulation, as shown in Fig. 6. This can slightly affect the lateral velocity of EC, and leave behind slight variation of poly-Si surface morphology and resulting macroscopic stripe patterns.

The variation of the surface morphology of a poly-Si film is actually confirmed in Fig. 7. Another fact we should mention here is that the temperature of a Si film decreases quickly after finishing the irradiation of flash-lamp pulse. For instance, the temperature of an a-Si film becomes less than 900 °C just 1 ms after stopping flash-pulse irradiation. Thus, slow crystallization of Si during cooling duration is unlikely, and crystallization is expected to take place during flash-pulse irradiation.

3.2 Characterization of FLC poly-Si films

Figure 8 shows the surface photographs of FLC poly-Si films formed from 10- and 3.5-μm-thick EB-evaporated a-Si films, respectively. One can see macroscopic stripe patterns on the surfaces of the FLC poly-Si films. The widths of the stripe patterns in the two figures are, however, significantly different even formed by sub-pulse emission with a same frequency of 5 kHz. This means that different types of EC take place, in spite of using a-Si films prepared under the same deposition conditions. Figure 9 shows the average width of macroscopic stripe patterns formed on FLC poly-Si films as a function of the inverse of sub-pulse emission frequency. The plots can be clearly separated into two groups, and the slopes of the plots, corresponding to the lateral EC velocity, are ~14 and ~4 m/s, respectively. According to our previous work, the former indicates the emergence of LPE-based EC which forms several tens of μm-long large grains [11], while the latter corresponds to the emergence of EC leaving behind SPN fine grains and 1-μm-spacing microscopic periodic structures [6]. We have so far reported that LPE-based EC tends to occur when EB-evaporated a-Si films are used as precursor a-Si films [11]. However, in the case of much thicker EB-evaporated a-Si films, slow EC becomes dominant. Figure 10 shows the cross-sectional TEM image of

a 10-μm-thick FLC poly-Si film formed from an EB-evaporated a-Si film. Particular periodic structures, whose spacing is approximately 1 μm, are clearly seen inside the poly-Si. The entire microstructure is quite similar to those of FLC poly-Si films formed from Cat-CVD and sputtered a-Si films [6,14], and thus, similar EC is likely to occur in a 10-μm-thick EB-evaporated poly-Si film. The formation of the periodic structures results from the alternative emergence of a LPE-dominant region and a SPN-dominant region [6]. It should be noted that there is no remarkable morphology change on the surface of a FLC poly-Si film formed from an EB-evaporated a-Si film, unlike the cases of using Cat-CVD or sputtered precursor films. This is probably related to film stress which precursor a-Si films originally have. Cat-CVD and sputtered films used in this study have a large compressive stress. In the present EC mode, part of Si is melted during the EC [6], and the melted Si is pushed up by receiving the compressive stress. On the other hand, EB-evaporated a-Si films have tensile stress [9,15], and the formation of roughened structures is suppressed even through the partial melting process. We should mention again here that the emergence of different types of EC can be clearly observed by the multi-pulse method.

Finally, we discuss the reason of the emergence of the different types of EC. We have so far already observed two types of EC, and clarified that LPE-based EC occurs when EB-evaporated precursor a-Si films are used [6,9,11]. We considered that its possible reason may be related to film stress [11]. However, 10-μm-thick EB-evaporated a-Si films show the EC similar to that of Cat-CVD and sputtered films, in spite of deposition conditions exactly same as a-Si films with a thickness of 3.5 μm. We have also confirmed that 4.5-μm-thick Cat-CVD a-Si films with a large (~200 MPa) tensile stress, formed by tuning deposition conditions, show ECs similar to the case of

compressively-stressed a-Si films [16]. These facts indicate that the stress of a-Si films is not a dominant factor to determine the EC mode. To discuss the ECs, we should consider two a-Si temperatures: 1) a temperature of ignition point (T_{ig}) and 2) a temperature of surrounding a-Si (T_{sur}). EC is thought to be ignited at a particular, almost constant T_{ig}. It is readily considered that LPE-based EC tends to occur at higher T_{sur}, because a thin liquid Si layer between a-Si and c-Si exists stably during the EC, while the other SPN-involved EC occurs at lower T_{sur} since the liquid Si region iteratively appears and disappears. We can thus expect that the T_{sur} in the case of LPE-based EC is much higher than T_{sur} for SPN-involved EC at the moment of the ignition. When we compare the cases of 3.5-μm-thick and 10-μm-thick EB-evaporated a-Si films, lower T_{sur} is realized in 10-μm-thick films at the instant of EC ignition. This is probably because of higher possibility of additional local heating in thicker a-Si films. Thicker a-Si films can receive more light on their film edges due to the existence of angled flash lamp light irradiation [6], at which EC is ignited more easily. Moreover, void-like structures in a-Si films can also be a cause of local heating, because downward thermal diffusion is suppressed by them. Thicker films can contain more void-like structures per unit area than thinner films, and are thus more favorable to ignite EC at lower temperature. It should also be mention that EC in EB-evaporated a-Si films tends to be ignited at higher T_{sur} than the other films, since LPE-based EC is not observed in Cat-CVD or sputtered films with a thickness of less than 3.5 μm [5,13]. This may be related to the presence or absence of gas component in precursor a-Si films. Sputtered and Cat-CVD a-Si films contain a large amount of Ar and H, respectively [7,13]. These gas components can accumulate locally and form void-like structures, which leads to the suppression of vertical thermal diffusion and the enhancement of the

ignition of EC. On the contrary, EB-evaporated a-Si films are deposited under low pressure, and much fewer gas impurities are captured. The ignition of EC thus tends to occur at higher T_{sur}, resulting in the emergence of LPE-based EC. Another important fact is that the EC modes are independent of flash pulse fluence, as far as we have attempted in a series of experiments. One may consider that the SPN-involved EC can shift to LPE-based EC under higher flash fluence. The unchanged EC mode is probably because EC occurs not after but in the middle of millisecond pulse irradiation. EC is ignited when T_{ig} reaches at a certain value. Thus, the irradiation of flash pulse with higher fluence just results in the earlier ignition of EC but not leads to the emergence of LPE-based EC.

4. Summary

Multi-pulse FLA, which emits a quasi-millisecond pulse light consisting of discrete sub-pulses, can be utilized to easily estimate lateral EC velocity without using any complicated *in-situ* measurement systems. Thermal simulation reveals that periodic temperature modulation is given to a-Si films by the irradiation of multi-pulse. Two kinds of ECs, whose EC velocities are 4 and 14 m/s, respectively, are observed depending on the thickness and deposition method of precursor a-Si films. The SPN-dominant EC leaving behind periodic microstructures can take place also in EB evaporated a-Si films when they are sufficiently thick. The emergence of different types of ECs can be understood as the ease of the ignition of EC depending on film thickness and gas components.

Acknowledgements

The author would like to thank L. Yang and S. Terashima of JAIST for their help to perform the thermal simulations and FLA experiments. The author also would like to acknowledge ULVAC Inc. for providing EB-evaporated a-Si films. This work was supported by JST PRESTO program.

References

1. J. Dore, D. Ong, S. Varlamov, R. Egan, and M. A. Green, IEEE J. Photovolt., (in press). doi: 10.1109/JPHOTOV.2013.2280016.
2. T. Matsuyama, M. Tanaka, S. Tsuda, S. Nakano, Y. Kuwano, Jpn. J. Appl. Phys., **32**, 3720 (1993). doi: 10.1143/JJAP.32.3720.
3. P. I. Widenborg, A. Straub, and A. G. Aberle, J. Cryst. Growth, **276**, 19 (2005). doi: 10.1016/j.jcrysgro.2004.10.155.
4. K. Ohdaira, S. Nishizaki, Y. Endo, T. Fujiwara, N. Usami, K. Nakajima, and H. Matsumura, Jpn. J. Appl. Phys., **46**, 7198 (2007). doi: 10.1143/JJAP.46.7198.
5. K. Ohdaira, Y. Endo, T. Fujiwara, S. Nishizaki, and H. Matsumura, Jpn. J. Appl. Phys., **46**, 7603 (2007). doi: 10.1143/JJAP.46.7603.
6. K. Ohdaira,T. Fujiwara, Y. Endo, S. Nishizaki, and H. Matsumura, J. Appl. Phys., **106**, 044907 (2009). doi: 10.1063/1.3195089.
7. K. Ohdaira, H. Takemoto, K. Shiba, and H. Matsumura, Appl. Phys. Express, **2**, 061201 (2009). doi: 10.1143/APEX.2.061201.
8. K. Ohdaira, T. Nishikawa, and H. Matsumura, J. Cryst. Growth **312**, 2834 (2010). doi: 10.1016/j.jcrysgro.2010.06.023.
9. K. Ohdaira, N. Tomura, S. Ishii, and H. Matsumura, Electrochem. Solid-State Lett., **14**, H372 (2011). doi: 10.1149/1.3602192.

10. K. Ohdaira, N. Tomura, S. Ishii, K. Sawada, and H. Matsumura, J. Non-Cryst. Solids, **358**, 2154 (2012). doi: 10.1016/j.jnoncrysol.2011.12.089.
11. K. Ohdaira and H. Matsumura, J. Cryst. Growth **362**, 149 (2013). doi: 10.1016/j.jcrysgro.2011.11.028.
12. T. Ito, K. Suguro, M. Tamura, T. Taniguchi, Y. Ushiku, T. Iinuma, T. Itani, M. Yoshioka, T. Owada, Y. Imaoka, H. Murayama, and T. Kusuda IEEE Trans. Semicond. Manuf., **16**, 417 (2003). doi: 10.1109/TSM.2003.815621.
13. H. -D. Geiler, E. Glaser, G. Götz, and M. Wagner, J. Appl. Phys. **59**, 3091 (1986). doi: 10.1063/1.336910.
14. K. Ohdaira, S. Ishii, N. Tomura, and H. Matsumura, J. Nanosci. Nanotech., **12**, 591 (2012). doi: 10.1166/JNN.2012.5342.
15. J. Kim, D. Inns, and D. K. Sadana, Thin Solid Films, **518**, 4908 (2010). doi: 10.1016/j.tsf.2010.03.161
16. K. Ohdaira, Thin Solid Films, (accepted)

Figure captions

Fig. 1 Sample structure and heating model for the thermal simulation. Irradiance of sub-pulses is 1.6 kW/cm^2, and the fluence of the quasi-5-ms pulse is 6.4 J/cm^2.

Fig. 2 FLA equipment used in this study. The lamp house can be moved from a detector position to a process chamber, and the fluence of a quasi-ms-pulse can be measured immediately before the flash irradiation to a sample.

Fig. 3 Photograph of a Xe lamp. A trigger electrode is wound around the Xe lamp. An impedance of Xe gas can be temporarily reduced by applying voltage to the trigger electrode.

Fig. 4 Photographs of pulse light seen between the lamp house and the process chamber at the moments of turning on and off the trigger voltage.

Fig. 5 Thermal simulation result of an a-Si/glass structure for heating by 4-kHz multi-pulse irradiation. Vertical and horizontal axes indicate depth and elapsed time, respectively. Temperature is indicated by color.

Fig. 6 Time-dependent temperature variations of the a-Si/glass structure at Si surface, Si bottom (glass surface), and glass bottom, respectively.

Fig. 7 Photograph of a FLC poly-Si film formed from a sputtered a-Si film and its surface microscopic images at different points.

Fig. 8 Surface photographs of FLC poly-Si films formed from (a) 10-μm-thick and (b) 3.5-μm-thick EB-evaporated a-Si films, respectively. Arrows indicate the widths of macroscopic stripe patterns formed by the multi-pulse irradiation.

Fig. 9 Average width of macroscopic stripe patterns formed on FLC poly-Si films as a function of the inverse of sub-pulse emission frequency.

Fig. 10 Cross-sectional TEM image of a FLC poly-Si film formed from a 10-μm-thick EB-evaporated a-Si film.

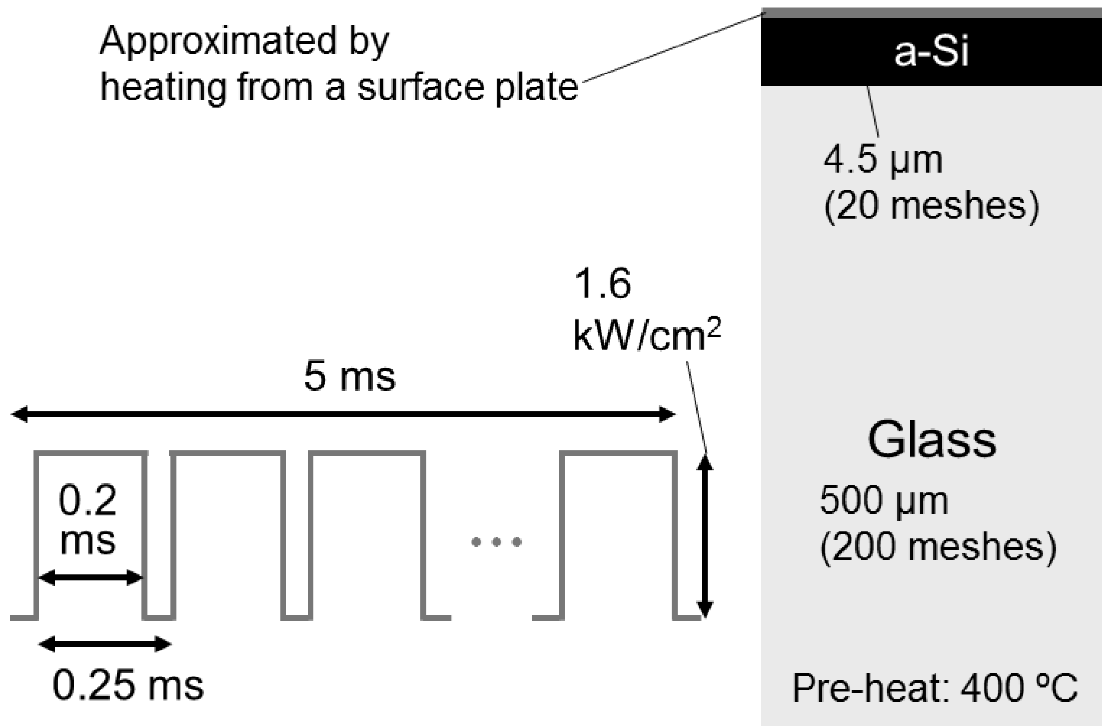
Approximated by
heating from a surface plate
a-Si
4.5 µm
(20 meshes)
1.6
kW/cm2
5 ms
0.2
ms
0.25 ms
Glass
500 µm
(200 meshes)
Pre-heat: 400 °C

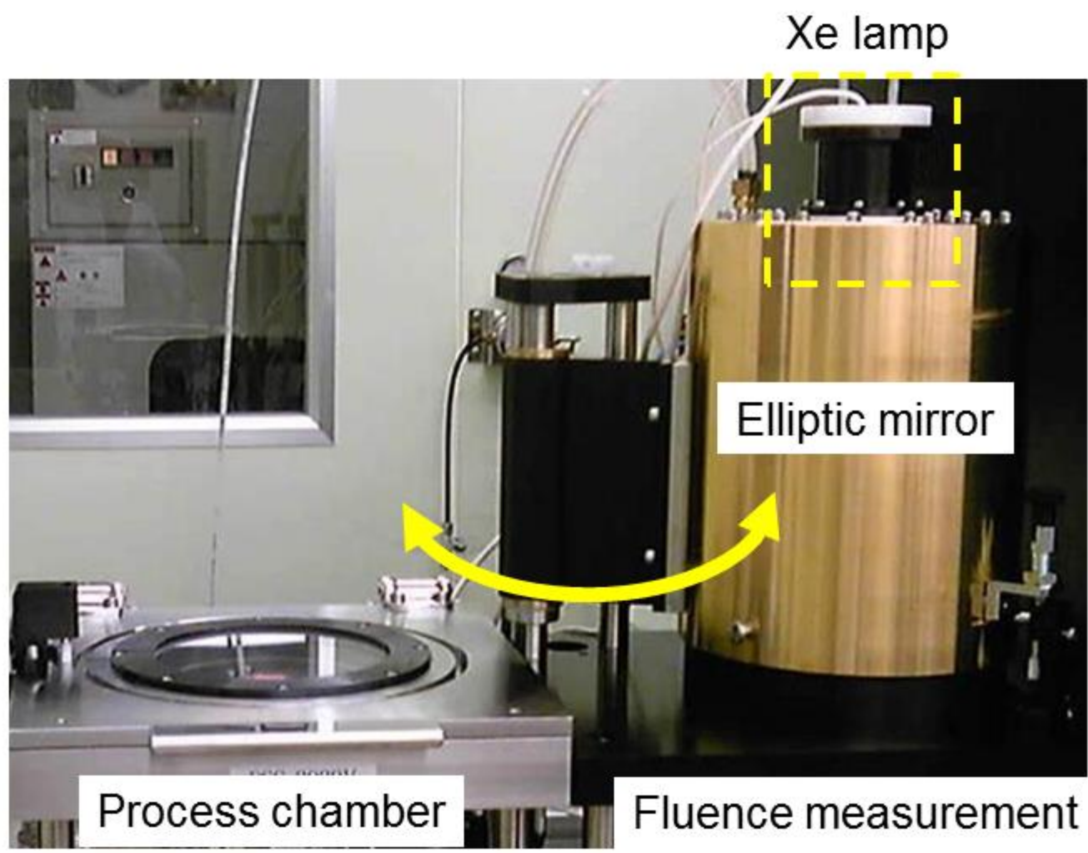
Xe lamp
Elliptic mirror
Process chamber
Fluence measurement

Electrodes
up to 1000 V
Trigger
electrode
1-10 kHz
15 kV

(a)

(b)

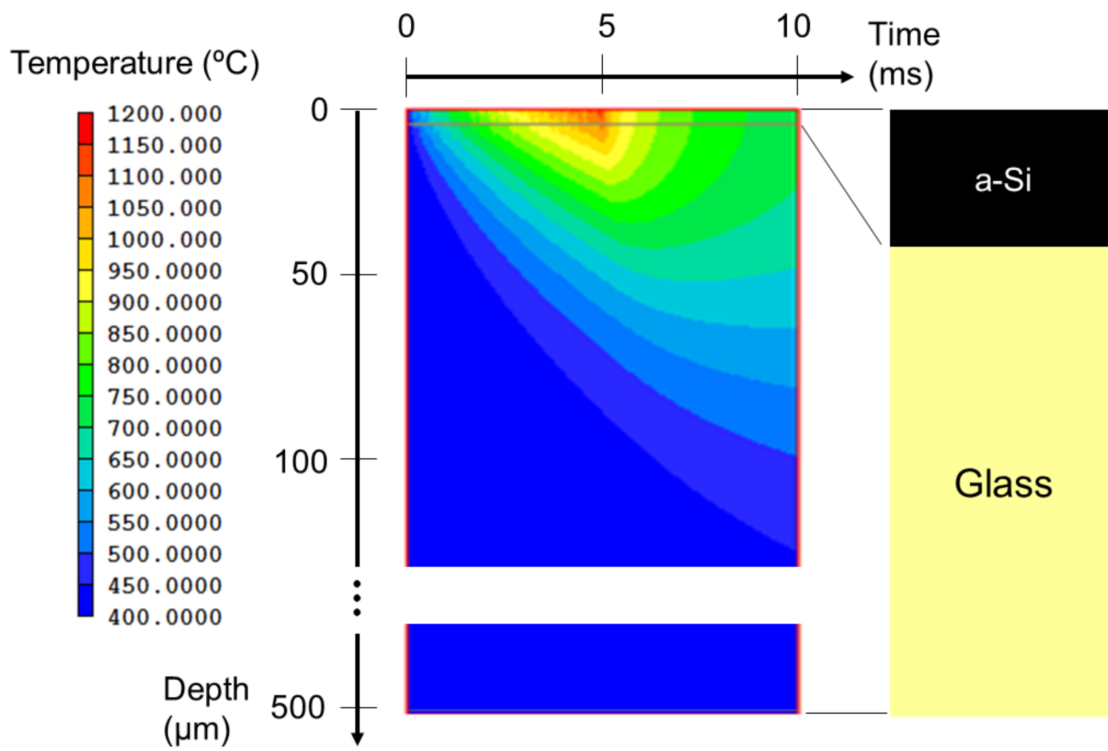

Temperature (ºC)
1200.000
1150.000
1100.000
1050.000
1000.000
950.0000
900.0000
850.0000
800.0000
750.0000
700.0000
650.0000
600.0000
550.0000
500.0000
450.0000
400.0000
0
5
10
Time (ms)
0
50
100
500
Depth (μm)
a-Si
Glass

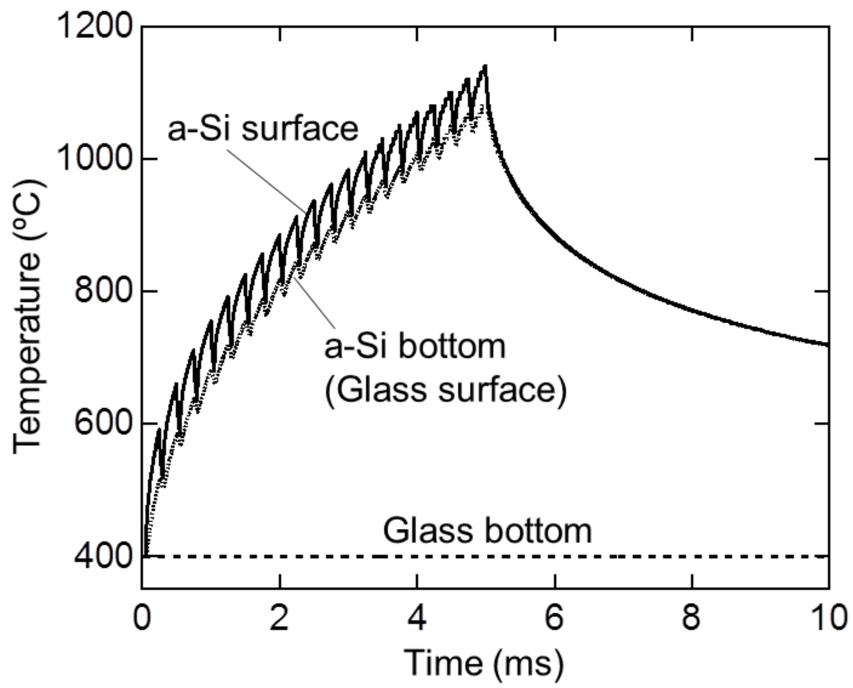
1200
1000
800
600
400
Temperature (ºC)
0
2
4
6
8
10
Time (ms)
a-Si surface
a-Si bottom
(Glass surface)
Glass bottom

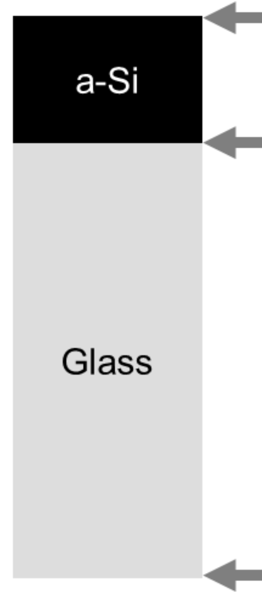
a-Si
Glass

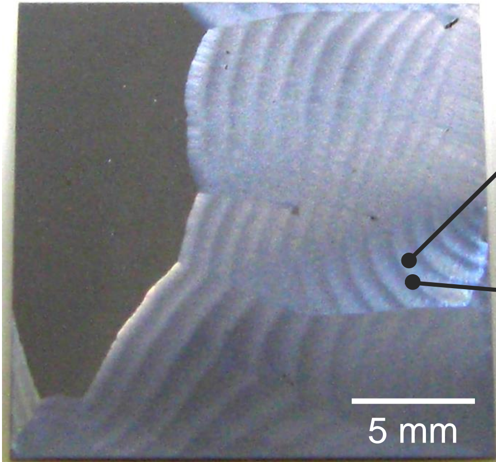
5 mm
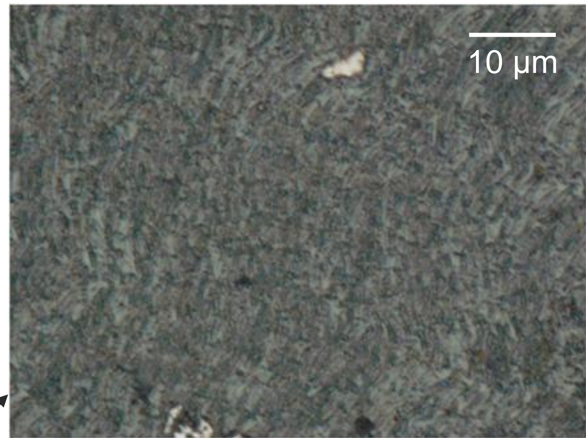
10 µm
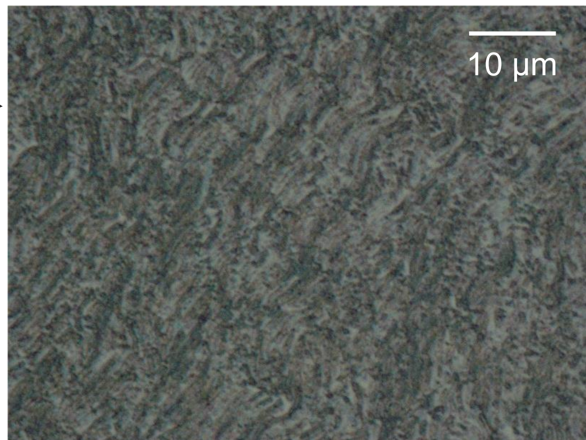
10 µm

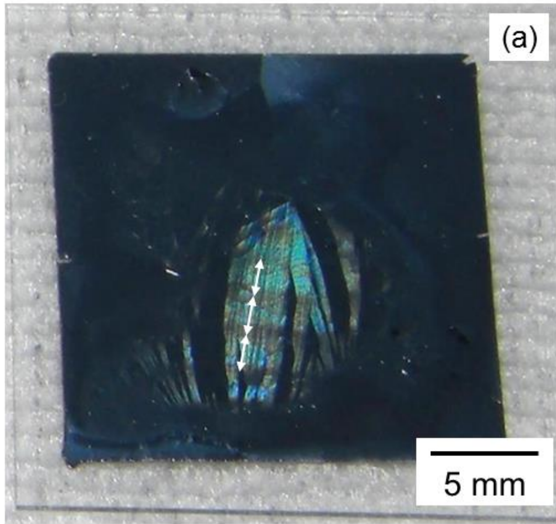
(a)
5 mm

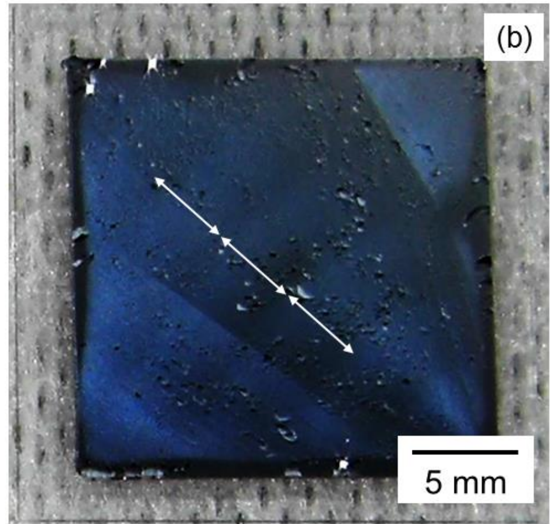
(b)
5 mm

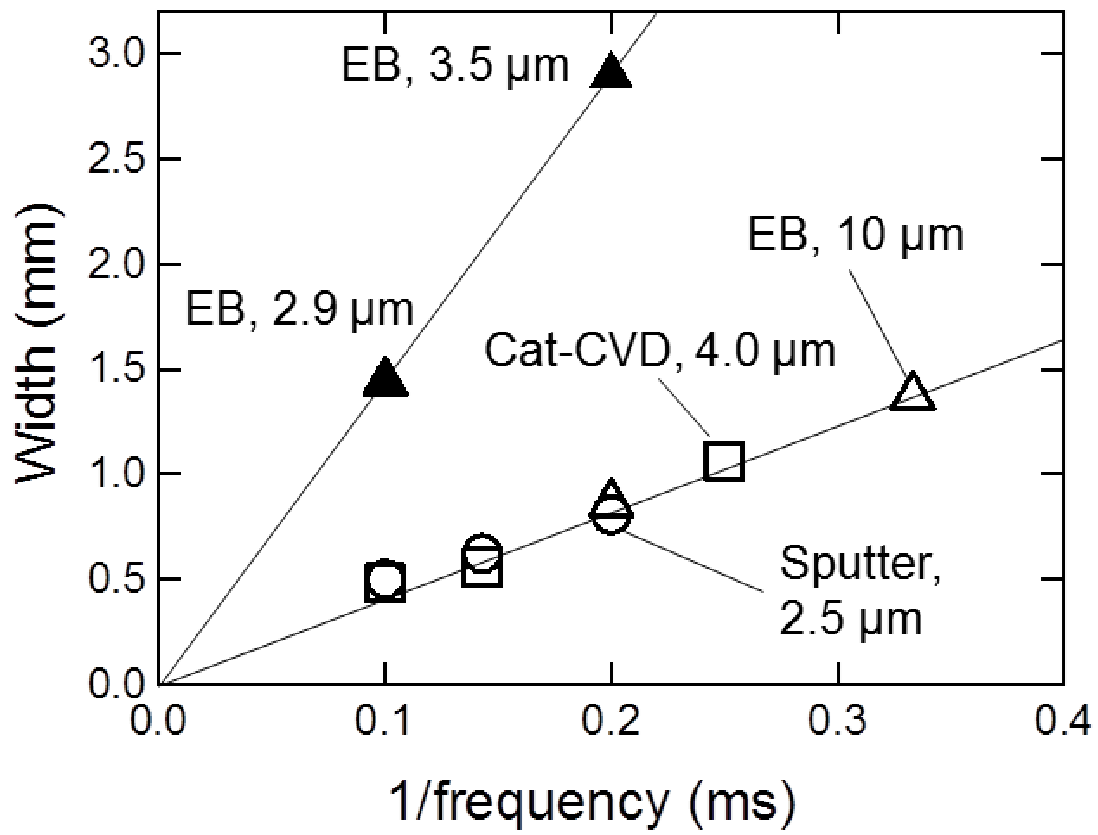

EB, 3.5 μm
EB, 2.9 μm
EB, 10 μm
Cat-CVD, 4.0 μm
Sputter,
2.5 μm
Width (mm)
1/frequency (ms)
0.0
0.5
1.0
1.5
2.0
2.5
3.0
0.0
0.1
0.2
0.3
0.4

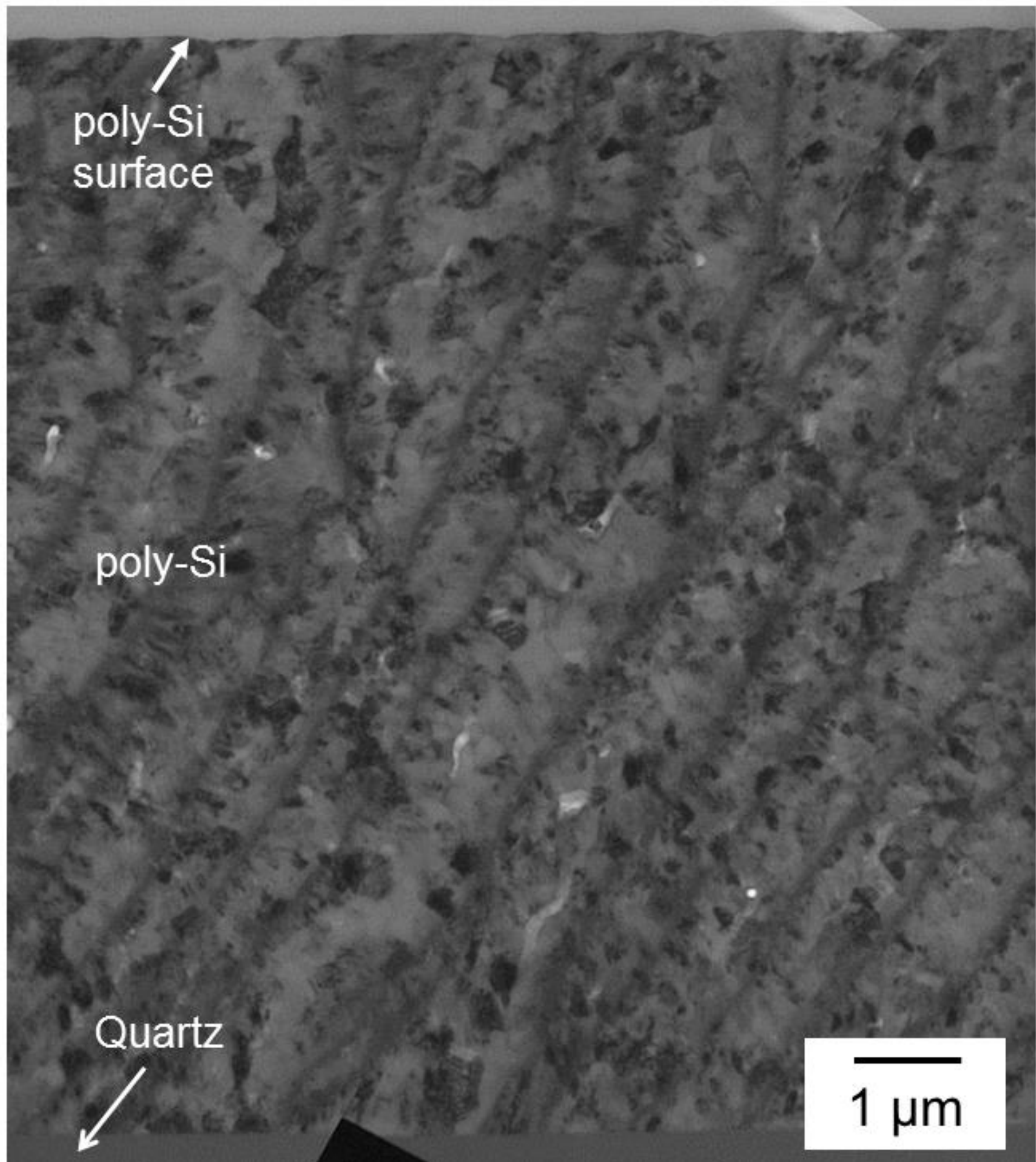
poly-Si
surface
poly-Si
Quartz
1 µm